

# Penetration of surface effects on structural relaxation and particle hops in glassy films

Qiang Zhai,<sup>1</sup> Hai-Yao Deng,<sup>2</sup> Xin-Yuan Gao,<sup>3</sup> Leo S.I. Lam,<sup>4</sup> Sen Yang,<sup>1,\*</sup> Ke Yan,<sup>5,†</sup> and Chi-Hang Lam<sup>6,‡</sup>

<sup>1</sup>MOE Key Laboratory for Nonequilibrium Synthesis and Modulation of Condensed Matter,  
School of Physics, Xi'an Jiaotong University, Xi'an, Shaanxi, 710049, China

<sup>2</sup>School of Physics and Astronomy, Cardiff University, 5 The Parade, Cardiff CF24 3AA, Wales

<sup>3</sup>Department of Physics, The Chinese University of Hong Kong, Shatin, New Territories, Hong Kong, China

<sup>4</sup>Department of Mechanical Engineering, Hong Kong Polytechnic University, Hong Kong, China

<sup>5</sup>School of Mechanical Engineering, Xi'an Jiaotong University, Xi'an, Shaanxi, 710049, China

<sup>6</sup>Department of Applied Physics, Hong Kong Polytechnic University, Hong Kong, China

(Dated: April 2, 2025)

A free surface induces enhanced dynamics in glass formers. We study the dynamical enhancement of glassy films with a distinguishable-particle lattice model of glass free of elastic effects. We demonstrate that the thickness of the surface mobile layer depends on temperature differently under different definitions, although all are based on local structure relaxation rate. The rate can be fitted to a double exponential form with an exponential-of-power-law tail. Our approach and results exclude elasticity as the unique mechanism for the tail. Layer-resolved particle hopping rate, potentially a key measure for activated hopping, is also studied but it exhibits much shallower surface effects.

## I. INTRODUCTION

It is well known that a glass former can retain a liquid-like free surface even though its bulk may well have vitrified [1–7]. Of films with free surfaces, a reduction in the glass transition temperature  $T_g$  accompanied by accelerated structural relaxation near the surface region has been observed [8–12]. Such surface-enhanced dynamics is confined to a surface mobile layer, over which local structural relaxation is accelerated. Its thickness has been studied in experiments [13–15] and simulations [16–21]. However, estimated values of the thickness and its temperature dependence can vary significantly among different definitions and are not yet fully understood.

A deeper question concerns the mechanism of the enhanced dynamics and the spatial functional form of its penetration into the interior of a film. It was argued that the local structural relaxation time, i.e.  $\alpha$ -relaxation time,  $\tau_\alpha(z)$  can shed light on the general question of the glass transition [22–29]. Here  $z$  is the depth from the free surface of a film. Yet, direct experimental tests of local properties against theoretical predictions are technically difficult, given the limited spatial resolution [23, 30]. Recently, accurate measurements of  $\tau_\alpha(z)$  from molecular dynamics (MD) simulations are reported to support a double-exponential form with an exponential-of-power-law tail given by [28]

$$\tau_\alpha^{-1}(z) = (\tau_\alpha^{\text{bulk}})^{-1} \exp[a \exp(-z/\xi_0) + b/z], \quad (1)$$

more often written as

$$\ln(\tau_\alpha^{\text{bulk}}/\tau_\alpha(z)) = a \exp(-z/\xi_0) + b/z, \quad (2)$$

where  $\xi_0$  measures the mobile layer thickness,  $\tau_\alpha^{\text{bulk}}$  is the bulk  $\alpha$ -relaxation time, and  $a$  and  $b$  are constants. Based on an

elastically cooperative nonlinear Langevin equation (ECNLE) theory [26], the double-exponential term, found also in early MD simulations [31], can be derived from an empirical layer-by-layer facilitation-like process for surface effects, while the tail can follow from a local softening due to an elastic coupling in three dimensions to the free surface [28]. Although the power-law tail covers only half a decade of scaling and may require further scrutiny, the intriguing two-component form seems evident from the accurate MD results. The functional form of Eq. (2) was claimed as a unique signature for the relevance of elastic field in glass [28]. This echoes a recent increase of interest [32, 33] in the possible dominating role of elasticity in glassy dynamics [34, 35].

Lattice models of glass in general enjoy superior computational efficiency [36, 37]. Here we use a distinguishable particle lattice model (DPLM) [38, 39] to study the relaxation dynamics of supported glassy films. The DPLM has been able to reproduce a variety of characteristic phenomena for bulk samples of glass, including slow relaxation [38], Kovacs paradox [40] and effect [41], kinetic and thermodynamic fragility [39], heat capacity overshoot [42], two-level systems [43], diffusion coefficient power-laws [44], and Kauzmann's paradox [45]. The same model has also successfully simulated surface enhanced mobility [46] and heat capacity [47] of glassy films. The importance of adopting an extensively tested lattice model is to ensure compatibility among explanations of a wide range of glassy phenomena. Mechanisms considered in this study based on the DPLM are thus also consistent with the aforementioned list of characteristics of glass in both bulk and film geometries.

In this paper, we measure and contrast estimates of the thickness of the surface mobile layer from DPLM simulations based on several commonly used definitions. We demonstrate that the local  $\alpha$ -relaxation time  $\tau_\alpha(z)$  measured for DPLM films can as well be fitted by Eq. (2), despite the absence of elastic effects. Finally, we show that the particle hopping rate from the DPLM admits much weaker surface enhancement than the relaxation time and the implications will be discussed.

\* yangsen@mail.xjtu.edu.cn

† yanke@mail.xjtu.edu.cn

‡ C.H.Lam@polyu.edu.hk

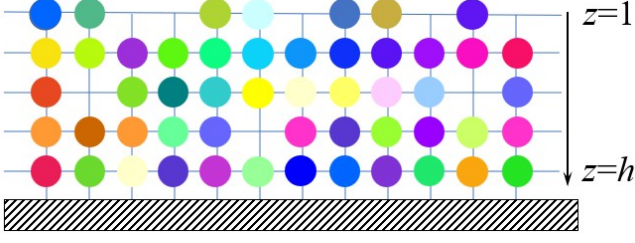


FIG. 1. A schematic drawing of the lattice model of supported film.

## II. MODEL

We follow the construction of DPLM films and all model parameters introduced previously for mobility and heat capacity measurements [46, 47]. Specifically,  $N$  distinguishable particles of each of their own type populate a square lattice of ribbon geometry, with thickness  $h$  and length  $L = 1000$ , in two dimensions (2D). Each lattice site can be occupied by either a particle or a void (non-occupied), as shown in Fig. 1. We apply periodic boundary conditions along the direction of  $L$  and fixed bounding walls along the direction of  $h$ . We designate  $z = 1$  for the particles in contact with the vacuum represented by the upper wall and  $z = h$  for the particles that sit on top of the substrate modeled by the lower wall. The energy of the model is given by

$$E = \sum_{\langle i,j \rangle} V_{s_i s_j} n_i n_j + \epsilon_{\text{bot}} \sum_{i:z_i=h} n_i + \epsilon_{\text{top}} \sum_{i:z_i=1} n_i. \quad (3)$$

Here, the particle type at the site  $i$  is labeled  $s_i$ . The interaction energy between the particle at the site  $i$  and the particle at the adjacent site  $j$  is given by  $V_{s_i s_j}$ . The occupation number  $n_i = 1$  at site  $i$  if site  $i$  is occupied by a particle, otherwise  $n_i = 0$  if the site is empty. The  $z$ -coordinate (i.e. depth) of site  $i$  is given by  $z_i$ . We use  $\epsilon_{\text{top}} = 1.124$  to account for the excess interfacial energy experienced by particles in  $z = 1$  and  $\epsilon_{\text{bot}} = -0.5$  for particles in  $z = h$ , respectively. We sample the interaction energy  $V_{s_i s_j}$  from a *a priori* distribution,

$$g(V) = G_0 / (V_1 - V_0) + (1 - G_0) \delta(V - V_1), \quad (4)$$

where  $V_0 = -0.5$ ,  $V_1 = 0.5$  and  $G_0 = 0.7$  are parameters chosen for the study [46].

We simulate void-induced equilibrium dynamics with the Metropolis algorithm. The rate for a particle hopping to an adjacent void is given by

$$w = w_0 \exp[-\Delta E \Theta(\Delta E) / k_B T], \quad (5)$$

where  $\Delta E$  is the energy change due to the hop,  $\Theta(x) = 1$  if  $x > 0$  or  $\Theta(x) = 0$  otherwise. We set the attempt frequency  $w_0 = 10^6$ . We use  $k_B = 1$ , so the temperature has the same dimension as energy. The adopted algorithm guarantees detailed balance.

We use the swap algorithm (swapping among all particles and voids) to accelerate the equilibration process [44, 48]. More than  $10^5$  swap attempts per site are performed to equilibrate the energy and depth-dependent particle density. Before

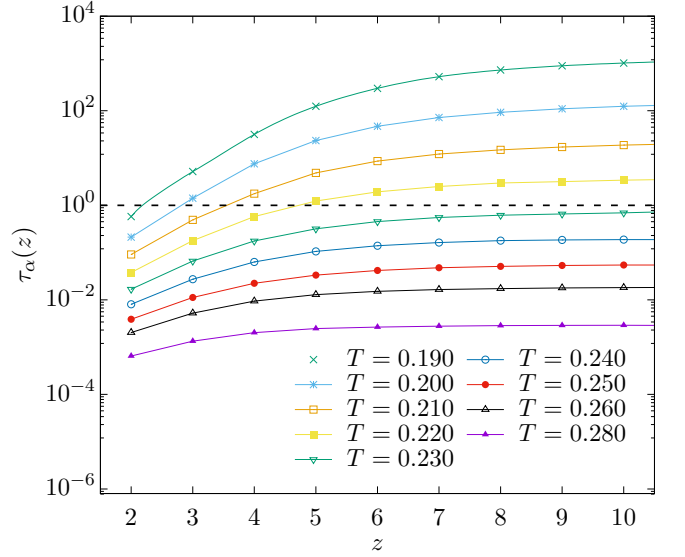


FIG. 2. Structural relaxation time,  $\tau_\alpha(z)$ , for a film of thickness  $h = 45$  at various values of temperature  $T$ . The free surface is adjacent to particles at  $z = 1$ . The dashed line sets an empirical reference observation time  $\tau_0 = 1$ .

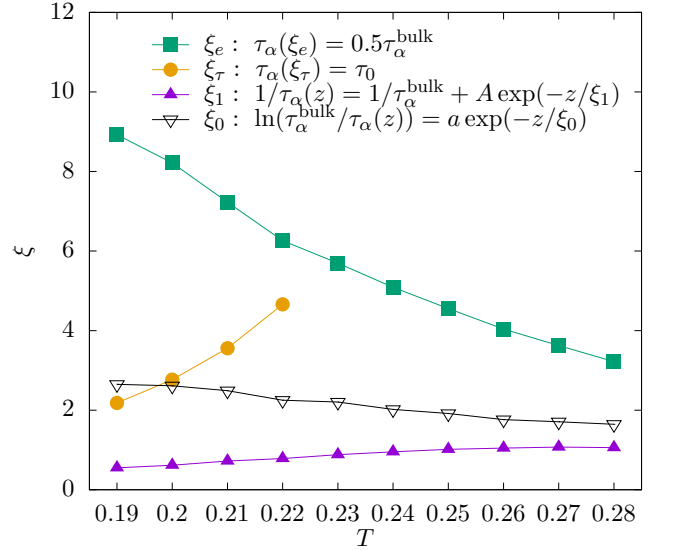


FIG. 3. Thicknesses of surface mobile layer based in different definitions against temperature  $T$  for a film of  $h = 45$ .

taking measurements, another  $10^5$  swap attempts per site are performed to confirm that equilibrium has been attained. With the parameters chosen above, it has been shown [46] that the particle density at  $z > 1$  equilibrates at a constant value of 0.99, and drops sharply to 0.2 at  $z = 1$ .

### III. RELAXATION RATE AND MOBILE LAYER THICKNESS

We measure from DPLM simulations the local overlap function  $q(\Delta t, z)$ , which gives the probability that a particle in layer  $z$  is at the original position after a duration  $\Delta t$ . In Fig. 2, we display the layer-resolved relaxation time  $\tau_\alpha(z)$  defined via  $q(\Delta t, z) = 1/e$  at  $\Delta t = \tau_\alpha(z)$  [46]. As seen, a slope of  $\tau_\alpha(z)$  extends towards the bulk and increases as  $T$  is reduced from 0.28 to 0.19. This is consistent with MD simulations [16] and signifies the penetration of fast surface dynamics into the interior of the film.

Using  $\tau_\alpha(z)$  from Fig. 2, we calculate the mobile layer thickness  $\xi_0$  from the double-exponential term in Eq. (2). Alternatively, we define a different mobile layer thickness  $\xi_\tau$  according to [14, 18, 27],

$$\tau_\alpha(\xi_\tau) = \tau_0, \quad (6)$$

based on an empirical reference relaxation time  $\tau_0$ . We have used  $\tau_0 = 1$ . In addition, one may introduce a third definition of thickness  $\xi_e$  according to [17, 18, 20]

$$\tau_\alpha(\xi_e) = 0.5\tau_\alpha^{\text{bulk}}, \quad (7)$$

where the mobility enhancement is gauged by the empirical prefactor 0.5 for the reduction of the relaxation time from the bulk value  $\tau_\alpha^{\text{bulk}}$ . Finally, from the gradient of  $\tau_\alpha(z)$  close to the free surface, we define a width  $\xi_1$  by a single-exponential form [21]

$$\tau_\alpha(z)^{-1} = (\tau_\alpha^{\text{bulk}})^{-1} + Ae^{-z/\xi_1}. \quad (8)$$

Figure 3 plots DPLM results on the thicknesses described above. As temperature decreases, we observe that  $\xi_\tau$  and  $\xi_1$  decrease while  $\xi_0$  and  $\xi_e$  increase. The temperature dependence of  $\xi_\tau$ ,  $\xi_0$ , and  $\xi_e$  has been studied before. Specifically, experiments on  $\xi_\tau$  [14] and MD results on  $\xi_\tau$  [18],  $\xi_0$  [31] and  $\xi_e$  [17, 18, 20] have all reported trends in good agreement with those from the DPLM in Fig. 3.

To further analyze the functional form of  $\tau_\alpha(z)$ , we have measured  $\tau_\alpha(z)$  from supported DPLM films of thickness  $h = 100$ . We determine  $\tau_\alpha^{\text{bulk}}$  accurately from simulations of bulk samples so that statistical errors are dominated by those of  $\tau_\alpha(z)$ . Figure 4 plots  $\log(\tau_\alpha^{\text{bulk}}/\tau_\alpha(z))$  against  $z$ . The result strikingly resembles those from recent MD measurements [28] and can be reasonably fitted to Eq. (2) with a double-exponential form in the short range and an upward-turning tail at  $z \gtrsim 30$ . Nevertheless, other functional forms may also be possible (see Appendix A).

### IV. WEAK SURFACE EFFECTS ON PARTICLE HOPS

Despite strong surface effects on the relaxation time, we next show that they are much weaker on particle hopping rate. At deep supercooling, particle dynamics in glass formers are dominated by activated particle hops as revealed by the emergence of secondary and higher-order peaks in the van Hove

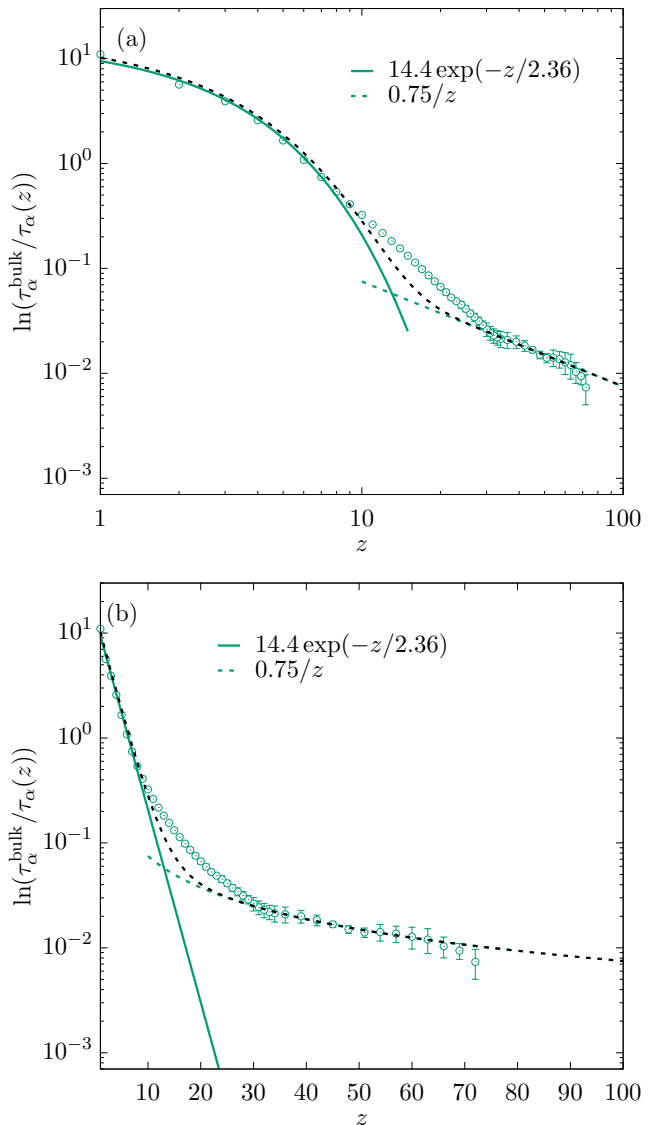


FIG. 4. Plot of  $\ln(\tau_\alpha^{\text{bulk}}/\tau_\alpha(z))$  versus depth  $z$  in (a) log-log and (b) semi-log scales for a film of thickness  $h = 100$  at  $T = 0.21$ . Two asymptotic fits to the data are also displayed. The black line indicates the sum of the two fits.

correlation function [49]. We now analyze the particle hopping rate defined by [21],

$$R_1(z) = \frac{P_{\text{hop}}(\Delta t, z)}{\Delta t}. \quad (9)$$

Here,  $P_{\text{hop}}(\Delta t, z)$  denotes the probability that a particle at layer  $z$  hops during a time interval  $\Delta t$  and is given by

$$P_{\text{hop}}(\Delta t, z) = \langle \Theta(|\mathbf{r}_i(t + \Delta t) - \mathbf{r}_i(t)| - 1) \rangle_{t,z}, \quad (10)$$

where  $\Theta(x) = 1$  if  $x \geq 0$ ,  $\mathbf{r}_i(t)$  is the position of particle  $i$  at time  $t$  and the average is taken over time  $t$  and all the particles that reside at depth  $z$  at the beginning of the time interval. We take a small time interval  $\Delta t = 10^{-7}$  so that  $R_1(z)$  measures the rate of all particle hops, as justified in Appendix B.

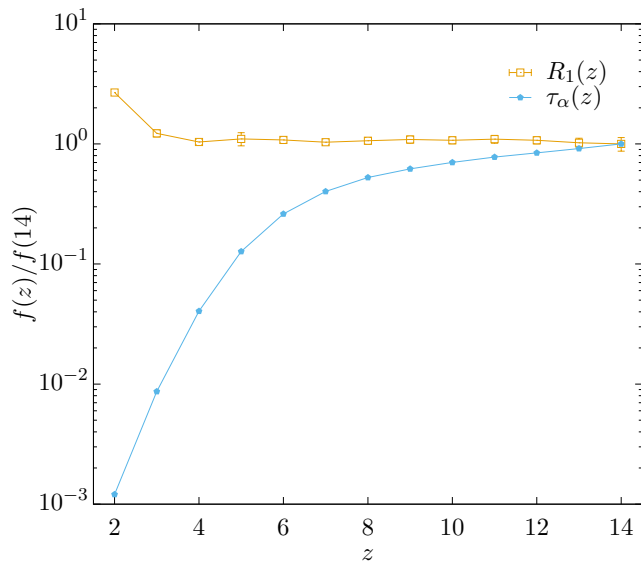


FIG. 5. Particle hopping rate  $R_1(z)$  against depth  $z$  for a film of thickness  $h = 15$  at temperature  $T = 0.20$ . Also plotted is structural relaxation time  $\tau_\alpha(z)$  under the same conditions. The data is normalized by the respective quantity at  $z = 14$ .

Fig. 5 displays  $R_1(z)$  measured against  $z$  from DPLM simulations at a low temperature of  $T = 0.20$ . It is compared with  $\tau_\alpha(z)$  reported above and values have been normalized by their approximate bulk values taken at  $z = 14$ . A clear difference between the strengths of the surface effects is seen. Specifically,  $\tau_\alpha(z)$  forms a gradient penetrating deep into the interior of the film up to at least  $z \simeq 13$ . In contrast, a gradient in  $R_1(z)$  extends only up to  $z \simeq 3$ .

In addition, the local particle density in the DPLM also admits surface effects only very close to the surface up to  $z \simeq 3$  [46], in qualitative agreement with MD results [16]. The behaviors of  $R_1(z)$  and the particle density are thus similar in this regard. This can be readily understood from the short-range nature of the interactions in the DPLM so that hopping energy barriers depend only on the local particle density. The deeper penetration of surface effects on relaxation time, not accountable by the particle hopping rate, has been attributed to a breakdown of a back-and-forth hopping tendency of glass particles close to the free surface [21].

## V. DISCUSSIONS

We have measured surface mobile layer thicknesses  $\xi_0$ ,  $\xi_\tau$ ,  $\xi_e$ , and  $\xi_1$  defined in Eqs. (2), (6), (7), and (8) respectively. Our results show that  $\xi_\tau$  and  $\xi_1$  increase with temperature, while  $\xi_0$  and  $\xi_e$  decrease with temperature. Such opposite trends are consistent with previous studies as explained above and have been discussed based on Adam-Gibbs theory [18] and cooperative free volume theory [27]. The reproduction of these trends here further supports the applicability of the DPLM on surface-enhanced dynamics in glassy films [46, 47], in addition to several other glassy phenomena demonstrated

previously [39–45].

The different properties of the various thicknesses demonstrate that a full characterization of surface enhanced mobility in general requires the whole function of layer-resolved relaxation time  $\tau_\alpha(z)$ , while an individual thickness reflects only certain features of the dynamics. In particular,  $\xi_e$  captures the length scale over which the system cannot maintain its bulk dynamics. It may be most closely related to the dynamic correlation length of glass in bulk, which is expected to increase as temperature decreases. In contrast,  $\xi_1$  is a decay length of enhanced dynamics close to the surface. It dictates the length scale of the layer dominating surface flow and is thus most relevant for quantifying surface transport [10, 19]. Its value decreases as temperature decreases, signifying that transport is dominated by an increasingly thinner layer.

The ENCLE theory based on elastic interactions [35] is an insightful analytical approach used in deriving Eq. (2), providing extensive microscopic details essential for close comparisons with MD simulations and other descriptions of glass relaxation. The exponential-of-power-law tail was taken as a unique signature of a long-range elastic field [28]. The fact that it is seen in Fig. 4 for the DPLM without elasticity calls into question such a feature as decisive evidence for the elastic picture.

Both the DPLM and the ENCLE theory can account for the exponential-of-power-law tail in the relaxation time, but they essentially produce opposite predictions on the particle hopping rate. We have observed in Fig. 5 surface effects on particle hopping rate in the DPLM only in a thin surface layer in agreement with our MD results [21]. Correlations among particle hops are known to play an important role [38]. In contrast, the ENCLE theory analyzes dynamics dictated by particle activated hopping energy barriers, while correlations among hops are completely neglected. The calculations essentially extract the structural relaxation rate directly from particle hopping rate. This should predict surface effects on relaxation rate penetrating as deep as those on hopping rates. It is not clear how the ENCLE theory can be reconciled with MD results in [21].

To conclude, we have measured from DPLM simulations the temperature dependence of four definitions of surface mobile layer thickness in glassy films. Different trends are observed in agreement with previous studies and they follow from different characteristics of the layer-resolved relaxation time. We also study the relaxation time including regions deep into the film. A two-component form with a slowly decaying tail closely resembling accurate MD measurements is observed. Our results show that long-range elastic interactions, which are absent in the DPLM, are not a necessary explanation of the tail. We also demonstrate that the particle hopping rate admits much shallower surface effects in the DPLM, again in agreement with MD simulations.

## ACKNOWLEDGMENTS

This work was supported by China Postdoc Fund Grant No. 2022M722548, Shaanxi NSF Grant No. 2023-JC-

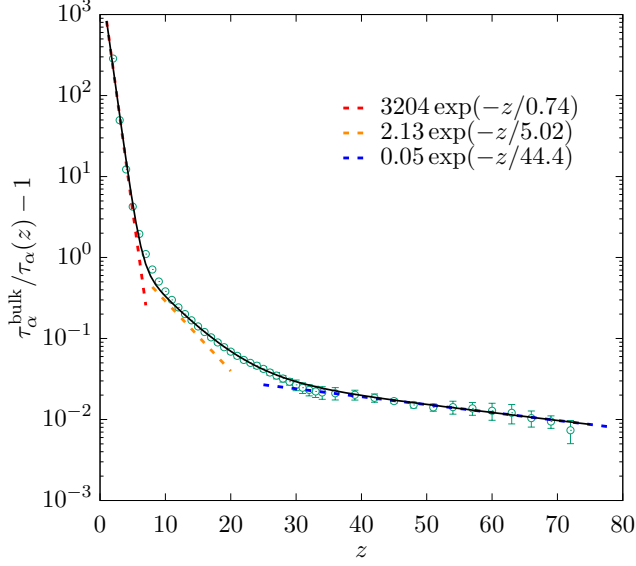


FIG. 6.  $\tau_\alpha^{\text{bulk}}/\tau_\alpha(z) - 1$  plotted against  $z$  using the same data in Fig. 4. The red, orange and blue lines are three asymptotic exponential fits to the data. The black line, sum of the three fits, displays a good agreement with the simulation data.

QN-0018, Central University Basic Research Fund Grant No. xzy012023044, National Natural Science Foundation of China Grant No. 12405042, Hong Kong GRF Grant No. 15303220.

#### DATA AVAILABILITY STATEMENT

The data that support the findings of this study are available from the corresponding author upon reasonable request.

#### Appendix A: Relaxation enhancement as a sum of exponentials

Figure 6 presents the data of  $\tau_\alpha(z)$  from Fig. 4 fitted to an empirical sum of three exponentials

$$\tau_\alpha^{-1}(z) = (\tau_\alpha^{\text{bulk}})^{-1} + A_1 e^{z/\xi_1} + A_2 e^{z/\xi_2} + A_3 e^{z/\xi_3}. \quad (\text{A1})$$

which generalizes Eq. (8). The three exponential terms are simplified effective forms to account for possible mobility enhancement induced respectively by isolated voids exchanged with the surface, coupled voids exchanged with the surface, and all coupled voids, as motivated by simulation results using a facilitated random walk model to be reported elsewhere. At present, the finite precision of our data in Fig. 6 and the large number of fitting parameters forbid us to scrutinize Eqs. (2) and (A1) reliably.

#### Appendix B: Further results on particle hopping rate

A layer-resolved particle hopping rate  $R_1(z)$  has been defined in Eq. (9). Following a definition applied previously to

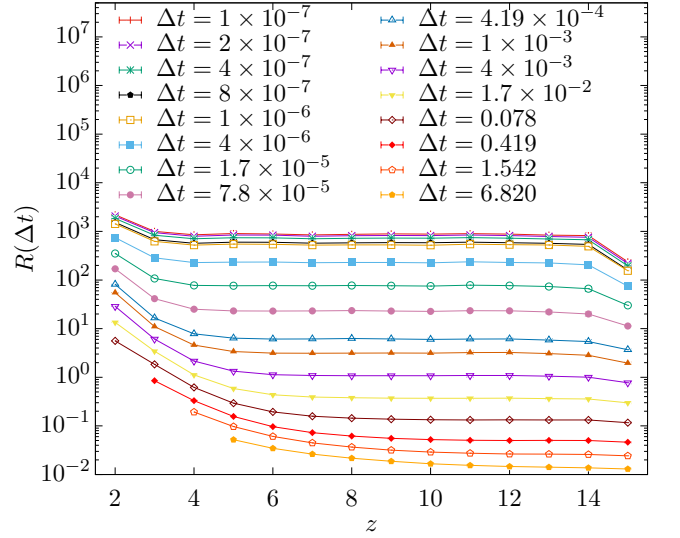


FIG. 7. Net hopping rates  $R(\Delta t)$  against depth  $z$  for a film of thickness  $h = 15$  at different values of  $\Delta t$  at  $T = 0.20$ .

MD results [21], it is generalized to a net hopping rate

$$R(z, \Delta t) = \frac{P_{\text{hop}}(\Delta t, z)}{\Delta t}, \quad (\text{B1})$$

where  $P_{\text{hop}}(\Delta t, z)$  defined in Eq. (10) denotes the probability that a particle at depth  $z$  hops during time  $\Delta t$ . For a very small time interval  $\Delta t = 10^{-7}$ , the hopping rate  $R_1(z)$  is restored. Figure 7 plots results on  $R(z, \Delta t)$  for different  $\Delta t$  from DPLM simulations. Note that we have ensured that  $\Delta t$  is small enough by showing only data points for which  $P_{\text{hop}}(\Delta t, z) \leq 0.5$ . The results in Fig. 7 qualitatively resemble those from MD simulations [21]. For  $\Delta t \simeq 10^{-7}$ ,  $R(z, \Delta t)$  have approximately converged and this signifies that all hops are properly counted. In contrast,  $R(z, \Delta t)$  decreases with  $\Delta t$  at larger  $\Delta t$ . This is because back-and-forth hops, which are very abundant in the system, then do not contribute to  $R(z, \Delta t)$ , properly reflecting that they also do not contribute to the net dynamics at longer time scales as explained in [21]. In particular, the gradient in  $R(z, \Delta t)$  penetrates deeper into the bulk for larger  $\Delta t$ . More precisely,  $R(z, \Delta t)$  at  $\Delta t = 6.820$  converges to its bulk value at  $z \gtrsim 12$ , in sharp contrast to  $R_1(z)$  which converges at a much shallower depth of  $z \gtrsim 3$ . This exemplifies that surface effects for long-time measurements such as  $R(z, \Delta t)$  for large  $\Delta t$  and  $\tau_\alpha(z)$  penetrate deeper than short-time values such as  $R_1(z)$  [21].

- [1] J. Baschnagel and F. Varnik, Computer simulations of supercooled polymer melts in the bulk and in confined geometry, *Journal of Physics: Condensed Matter* **17**, R851 (2005).
- [2] M. D. Ediger and J. A. Forrest, Dynamics near free surfaces and the glass transition in thin polymer films: a view to the future, *Macromolecules* **47**, 471 (2013).
- [3] S. Napolitano, E. Glynos, and N. B. Tito, Glass transition of polymers in bulk, confined geometries, and near interfaces, *Reports on Progress in Physics* **80**, 036602 (2017).
- [4] G. B. McKenna and S. L. Simon, 50th anniversary perspective: Challenges in the dynamics and kinetics of glass-forming polymers, *Macromolecules* **50**, 6333 (2017).
- [5] C. B. Roth, Polymers under nanoconfinement: where are we now in understanding local property changes?, *Chemical Society Reviews* **50**, 8050 (2021).
- [6] C. Rodriguez-Tinoco, M. Gonzalez-Silveira, M. A. Ramos, and J. Rodriguez-Viejo, Ultrastable glasses: new perspectives for an old problem, *La Rivista del Nuovo Cimento* **45**, 325 (2022).
- [7] D. Cangialosi, Physical aging and vitrification in polymers and other glasses: Complex behavior and size effects, *Journal of Polymer Science* **62**, 1952 (2024).
- [8] J. L. Keddie, R. A. L. Jones, and R. A. Cory, Size-dependent depression of the glass transition temperature in polymer films, *Euro. Phys. Lett.* **27**, 59 (1994).
- [9] Z. Fakhraai and J. A. Forrest, Measuring the surface dynamics of glassy polymers, *Science* **319**, 600 (2008).
- [10] Z. Yang, Y. Fujii, F. K. Lee, C.-H. Lam, and O. K. C. Tsui, Glass transition dynamics and surface layer mobility in unentangled polystyrene films, *Science* **328**, 1676 (2010).
- [11] L. Zhu, C. Brian, S. Swallen, P. Straus, M. Ediger, and L. Yu, Surface self-diffusion of an organic glass, *Physical Review Letters* **106**, 256103 (2011).
- [12] Y. Chai, T. Salez, J. D. McGraw, M. Benzaquen, K. Dalnoki-Veress, E. Raphaël, and J. A. Forrest, A direct quantitative measure of surface mobility in a glassy polymer, *Science* **343**, 994 (2014).
- [13] M. Ilton, D. Qi, and J. A. Forrest, Using nanoparticle embedding to probe surface rheology and the length scale of surface mobility in glassy polymers, *Macromolecules* **42**, 6851 (2009).
- [14] K. Paeng, S. F. Swallen, and M. D. Ediger, Direct measurement of molecular motion in freestanding polystyrene thin films, *Journal of the American Chemical Society* **133**, 8444 (2011).
- [15] H. Yuan, J. Yan, P. Gao, S. K. Kumar, and O. K. Tsui, Microscale mobile surface double layer in a glassy polymer, *Science Advances* **8**, eabq5295 (2022).
- [16] F. Varnik, J. Baschnagel, and K. Binder, Reduction of the glass transition temperature in polymer films: A molecular-dynamics study, *Physical Review E* **65**, 021507 (2002).
- [17] P. Z. Hanakata, J. F. Douglas, and F. W. Starr, Local variation of fragility and glass transition temperature of ultra-thin supported polymer films, *The Journal of Chemical Physics* **137**, 244901 (2012).
- [18] R. J. Lang and D. S. Simmons, Interfacial dynamic length scales in the glass transition of a model freestanding polymer film and their connection to cooperative motion, *Macromolecules* **46**, 9818 (2013).
- [19] C.-H. Lam and O. K. C. Tsui, Crossover to surface flow in supercooled unentangled polymer films, *Phys. Rev. E* **88**, 042604 (2013).
- [20] A. Shavit and R. A. Riggleman, Physical aging, the local dynamics of glass-forming polymers under nanoscale confinement, *The Journal of Physical Chemistry B* **118**, 9096 (2014), PMID: 25046680.
- [21] C.-H. Lam, Deeper penetration of surface effects on particle mobility than on hopping rate in glassy polymer films, *J. Chem. Phys.* **149**, 164909 (2018).
- [22] D. Long and F. Lequeux, Heterogeneous dynamics at the glass transition in van der Waals liquids, in the bulk and in thin films, *Eur. Phys. J. E* **4**, 371 (2001).
- [23] C. J. Ellison and J. M. Torkelson, The distribution of glass-transition temperatures in nanoscopically confined glass formers, *Nature Materials* **2**, 695 (2003).
- [24] J. E. Pye, K. A. Rohald, E. A. Baker, and C. B. Roth, Physical aging in ultrathin polystyrene films: Evidence of a gradient in dynamics at the free surface and its connection to the glass transition temperature reductions, *Macromolecules* **43**, 8296 (2010).
- [25] T. Salez, J. Salez, K. Dalnoki-Veress, E. Raphaël, and J. A. Forrest, Cooperative strings and glassy interfaces, *Proc. Natl. Acad. Sci.* **112**, 8227 (2015).
- [26] A. D. Phan and K. S. Schweizer, Theory of the spatial transfer of interface-nucleated changes of dynamical constraints and its consequences in glass-forming films, *J. Chem. Phys.* **150** (2019).
- [27] R. P. White and J. E. Lipson, Dynamics across a free surface reflect interplay between density and cooperative length: Application to polystyrene, *Macromolecules* **54**, 4136 (2021).
- [28] A. Ghanekarade, A. D. Phan, K. S. Schweizer, and D. S. Simmons, Signature of collective elastic glass physics in surface-induced long-range tails in dynamical gradients, *Nat. Phys.* **19**, 800 (2023).
- [29] C. Herrero and L. Berthier, Direct numerical analysis of dynamic facilitation in glass-forming liquids, *Phys. Rev. Lett.* **132**, 258201 (2024).
- [30] R. R. Baglay and C. B. Roth, Experimental study of the influence of periodic boundary conditions: Effects of finite size and faster cooling rates on dissimilar polymer-polymer interfaces, *ACS Macro Letters* **6**, 887 (2017).
- [31] P. Scheidler, W. Kob, and K. Binder, The relaxation dynamics of a confined glassy simple liquid, *The European Physical Journal E* **12**, 5 (2003).
- [32] A. Tahaei, G. Biroli, M. Ozawa, M. Popović, and M. Wyart, Scaling description of dynamical heterogeneity and avalanches of relaxation in glass-forming liquids, *Phys. Rev. X* **13**, 031034 (2023).
- [33] M. R. Hasyim and K. K. Mandadapu, Emergent facilitation and glassy dynamics in supercooled liquids, *Proceedings of the National Academy of Sciences* **121**, e2322592121 (2024).
- [34] J. C. Dyre, Colloquium: The glass transition and elastic models of glass-forming liquids, *Rev. Mod. Phys.* **78**, 953 (2006).
- [35] K. S. Schweizer and D. S. Simmons, Progress towards a phenomenological picture and theoretical understanding of glassy dynamics and vitrification near interfaces and under nanoconfinement, *J. Chem. Phys.* **151**, 240901 (2019).
- [36] J. P. Garrahan, P. Sollich, and C. Toninelli, Kinetically constrained models, in *Dynamical Heterogeneities in Glasses, Colloids and Granular Media*, edited by L. Berthier, G. Biroli, J.-P. Bouchaud, L. Cipelletti, and W. van Saarloos (Oxford University Press, 2011).
- [37] F. Ritort and P. Sollich, Glassy dynamics of kinetically constrained models, *Adv. Phys.* **52**, 219 (2003).

- [38] L.-H. Zhang and C.-H. Lam, Emergent facilitation behavior in a distinguishable-particle lattice model of glass, *Phys. Rev. B* **95**, 184202 (2017).
- [39] C.-S. Lee, M. Lulli, L.-H. Zhang, H.-Y. Deng, and C.-H. Lam, Fragile glasses associated with a dramatic drop of entropy under supercooling, *Phys. Rev. Lett.* **125**, 265703 (2020).
- [40] M. Lulli, C.-S. Lee, H.-Y. Deng, C.-T. Yip, and C.-H. Lam, Spatial heterogeneities in structural temperature cause Kovacs' expansion gap paradox in aging of glasses, *Phys. Rev. Lett.* **124**, 095501 (2020).
- [41] M. Lulli, C.-S. Lee, L.-H. Zhang, H.-Y. Deng, and C.-H. Lam, Kovacs effect in glass with material memory revealed in non-equilibrium particle interactions, *J. Stat. Mech.* **2021**, 093303 (2021).
- [42] C.-S. Lee, H.-Y. Deng, C.-T. Yip, and C.-H. Lam, Large heat-capacity jump in cooling-heating of fragile glass from kinetic monte carlo simulations based on a two-state picture, *Phys. Rev. E* **104**, 024131 (2021).
- [43] X.-Y. Gao, H.-Y. Deng, C.-S. Lee, J. You, and C.-H. Lam, Emergence of two-level systems in glass formers: a kinetic monte carlo study, *Soft Matter* **18**, 2211 (2022).
- [44] G. Gopinath, C.-S. Lee, X.-Y. Gao, X.-D. An, C.-H. Chan, C.-T. Yip, H.-Y. Deng, and C.-H. Lam, Diffusion-coefficient power laws and defect-driven glassy dynamics in swap acceleration, *Phys. Rev. Lett.* **129**, 168002 (2022).
- [45] X.-Y. Gao, C.-Y. Ong, C.-S. Lee, C.-T. Yip, H.-Y. Deng, and C.-H. Lam, Kauzmann paradox: A possible crossover due to diminishing local excitations, *Phys. Rev. B* **107**, 174206 (2023).
- [46] Q. Zhai, X.-Y. Gao, C.-S. Lee, C.-Y. Ong, K. Yan, H.-Y. Deng, S. Yang, and C.-H. Lam, Surface mobility gradient and emergent facilitation in glassy films, *Soft matter* **20**, 4389 (2024).
- [47] Q. Zhai, X.-Y. Gao, H.-Y. Deng, C.-S. Lee, S. Yang, K. Yan, and C.-H. Lam, Heat capacity and relaxation dynamics of glassy films: A lattice model study, *Phys. Rev. E* **111**, 015406 (2025).
- [48] A. Ninarello, L. Berthier, and D. Coslovich, Models and algorithms for the next generation of glass transition studies, *Phys. Rev. X* **7**, 021039 (2017).
- [49] T. Kawasaki and A. Onuki, Slow relaxations and stringlike jump motions in fragile glass-forming liquids: Breakdown of the stokes-einstein relation, *Phys. Rev. E* **87**, 012312 (2013).